

Synthesis, Molecular Modeling, and Biological Evaluation of Novel Chiral Thiosemicarbazone Derivatives as Potent Anticancer Agents

DEMET TAŞDEMİR,^{1*} AYŞEGÜL KARAKÜÇÜK-İYİDOĞAN,¹ MUSTAFA ULAŞLI,² TUĞBA TAŞKIN-TOK,¹ EMİNE ELÇİN ORUÇ-EMRE,¹ AND HASAN BAYRAM³

¹Gaziantep University, Faculty of Science and Arts, Department of Chemistry, Gaziantep, Turkey

²Gaziantep University, Faculty of Medicine, Department of Medical Biology, Sehitkamil, Gaziantep, Turkey

³Gaziantep University, Faculty of Medicine, Department of Pulmonary Diseases, Sehitkamil, Gaziantep, Turkey

ABSTRACT A series of new chiral thiosemicarbazones derived from homochiral amines in both enantiomeric forms were synthesized and evaluated for their in vitro antiproliferative activity against A549 (human alveolar adenocarcinoma), MCF-7 (human breast adenocarcinoma), HeLa (human cervical adenocarcinoma), and HGC-27 (human stomach carcinoma) cell lines. Some of compounds showed inhibitory activities on the growth of cancer cell lines. Especially, compound **17b** exhibited the most potent activity (IC₅₀ 4.6 μM) against HGC-27 as compared with the reference compound, sindaxel (IC₅₀ 10.3 μM), and could be used as a lead compound to search new chiral thiosemicarbazone derivatives as antiproliferative agents. *Chirality* 27:177–188, 2015. © 2014 Wiley Periodicals, Inc.

KEY WORDS: chiral amine; hydrazinecarbothioamide; cytotoxicity; HipHop; pharmacophore model

INTRODUCTION

Cancer is a significant cause of mortality and morbidity worldwide and current chemotherapeutic agents are not sufficiently effective. Delivery of anticancer drugs to specific tumor tissues is a complex process involving various biochemical, mechanical, and biophysical factors. Designing specific chemotherapeutic drugs may be challenging for treatment but using many advanced technologies such as next-generation sequencing, microarray protein expression profiles, and signaling pathways have supported the discovery of treatment targets and personalized treatments.¹ Recently, the majority of drugs used for cancer treatment are not "cancer cell-specific" and these drugs are cytotoxic for normal cells. Therefore, pharmaceutical research has depended on the discovery of new drugs for cancer treatment.²

Thiosemicarbazones are an important class of imine derivatives that have very different kinds of pharmacological activities, especially as anticancer agents.³ Their anticancer activity is attributed to the ability to inhibit three target points on which research is focused. First, thiosemicarbazone derivatives inhibit the iron-containing ribonucleotide reductase, which is involved in the biosynthesis of DNA by metal chelation.^{4–6} Second, these compounds inhibit topoisomerase II by stabilization of the cleavable complex between this enzyme and DNA through a thiol alkylation.^{7–9} Third, recently thiosemicarbazones were found to be inhibitors of ATP-binding cassette (ABC) transporters, which are known to play a critical role in the development of multidrug resistance.^{10,11}

Biological systems (proteins, sugars, enzymes, etc.) recognize an enantiomer pair as different substances and so two enantiomers of a chiral drug molecule bind differently to target receptors. Consequently, an enantiomer may act as an efficient therapeutic drug while the other enantiomer is inactive or highly toxic.^{12–14} Approximately 56% of the drugs currently in use are chiral compounds, and about 88% of these chiral synthetic drugs are used therapeutically as racemates. Unfortunately, there are many racemic drugs where the stereospecificity of the metabolism and/or the pharmacodynamic effects of the enantiomers is not known.¹⁵ Therefore, the synthesis

of chiral drugs in enantiopure form is very important in synthetic organic chemistry, medicinal chemistry, natural product chemistry, and the pharmaceutical industry.^{16,17} When a chiral compound is synthesized in several steps, it can be important for practical and economic reasons to introduce the proper stereochemistry at an early stage. This can be achieved starting from chiral building blocks that are enantiomerically pure and have functionalities that allow them to be transformed into the desired product.¹⁸ According to this approach, chiral amines can be considered convenient starting materials in the synthesis of chiral thiosemicarbazones because they are commercially available, and generally accessible in two enantiomeric forms.

In continuation of our research on compounds endowed with anticancer activity, we designed and synthesized enantiopure thiosemicarbazones derived from homochiral amines as chiral building blocks. Our previous results have shown that the reaction in basic media between amines and CS₂ in CHCl₃ is a very efficient procedure to synthesize the chiral isothiocyanate derivatives. Furthermore, this process retains the stereochemistry of the starting chiral amine. In the present work, we prepared chiral thiosemicarbazones with good yield and high enantiopurity and evaluated their cytotoxic activity against human alveolar adenocarcinoma (A549), human breast adenocarcinoma (MCF-7), human cervical adenocarcinoma (HeLa), and human stomach carcinoma (HGC-27) cell lines. In addition, a virtual screening of the mentioned chiral thiosemicarbazone (**17b**) was performed to illustrate its SAR (structure–activity relationships) of active sites of protein–ligand interactions and possible conformations by generating a pharmacophore hypothesis to increase knowledge of the structure and mechanism.

*Correspondence to: Demet Taşdemir, Gaziantep University, Faculty of Science and Arts, Department of Chemistry, 27310, Gaziantep, Turkey.
E-mail: demettasdemir@gmail.com

Received for publication 2 September 2014; Accepted 13 October 2014

DOI: 10.1002/chir.22408

Published online 14 November 2014 in Wiley Online Library (wileyonlinelibrary.com).

EXPERIMENTAL

Measurement and Reagents

Melting points were determined in an EZ-Melt MPA120 Automated Melting Point apparatus. The optical rotations were determined in a PoLAAr 3000 polarimeter at 20°C, using dimethyl sulfoxide (DMSO). UV-vis spectra were recorded on a PG Instruments (UK) T80+ UV-visible spectrophotometer in DMF. IR spectra were recorded on a Perkin Elmer (Boston, MA) 1620 model FT-IR Spectrophotometer with a universal ATR sampling accessory. ¹H and ¹³C nuclear magnetic resonance (NMR) spectra were obtained at room temperature with a Bruker (Billerica, MA) AVANC-DPX NMR spectrophotometer in DMSO-*d*₆ using tetramethylsilane (TMS) as an internal standard at 400 MHz and 100 MHz, respectively. The chemical shifts are given in parts per million (ppm) downfield from TMS. The splitting patterns of ¹H NMR were designed as follows: s: singlet, brs: broad singlet, d: doublet, dd: double doublet, t: triplet, q: quartet, p: pentet, m: multiplet. The coupling constants (*J*) are given in Hertz. The mass spectra were obtained using an ABSciex 3200 QTrap system liquid chromatography, tandem mass spectroscopy (LC/MS/MS) in the electrospray mode. Elemental analyses (CHNS) data were obtained by a Thermo Scientific (Pittsburgh, PA) Flash 2000 elemental analyzer.

All chemicals and solvents were purchased from Merck (Darmstadt, Germany) and Aldrich Chemical (Milwaukee, WI) and used without further purification. All reaction progress was monitored by thin layer chromatography (TLC). TLC was performed on silica gel plates (Merck Silica Gel 60, F₂₅₄, 0.2 mm) with visualization by exposure to iodine vapor and UV-light using EtOAc/hexane (v/v 1:1 and 1:3) as the solvent system.

Synthesis of Thiosemicarbazones 3a-17a and 3b-17b: A General Method

To a hot solution of chiral thiosemicarbazides **2a-2b** (1.53 mmol) in methanol (5 mL) was added dropwise a solution of the corresponding *p*-substituted benzaldehydes (1.53 mmol) in hot methanol (5 mL) over 15 min. The reaction mixture was refluxed and the progress of the reaction was followed by TLC (10–12 h) and cooled. The product was filtered and washed with petroleum ether. The crude product was recrystallized from ethanol.

(–)-(R)-N-(1-phenylethyl)hydrazinecarbothioamide (**2a**). Yellow viscous; yield 84%; IR (ν_{\max} , cm⁻¹): 3272 and 3092 (N-H), 1514 (C-N), 1191 (C=S); ¹H NMR (400 MHz, DMSO-*d*₆): δ 1.44 (d, 3H, *J* = 6.8 Hz, H-6'), 4.62 (brs, 2H, H-1), 5.55 (p, 1H, H-1'), 7.25 (t, 1H, *J*₁, *J*₂ = 6.8 Hz, H-5'), 7.30–7.35 (m, 4H, H-3', H-4'), 8.03 (d, 1H, *J* = 8.8 Hz, H-4), 8.74 (s, 1H, H-2).

(+)-(S)-N-(1-phenylethyl)hydrazinecarbothioamide (**2b**). Yellow viscous; yield 77%; IR (ν_{\max} , cm⁻¹): 3350 and 3157 (N-H), 1549 (C-N), 1128 (C=S); ¹H NMR (400 MHz, DMSO-*d*₆): δ 1.42 (d, 3H, *J* = 6.8 Hz, H-6'), 4.54 (brs, 2H, H-1), 5.51 (p, 1H, H-1'), 7.23 (t, 1H, *J*₁, *J*₂ = 6.8 Hz, H-5'), 7.24–7.37 (m, 4H, H-3', H-4'), 8.00 (d, 1H, *J* = 8.8 Hz, H-4), 8.68 (s, 1H, H-2).

(–)-(R)-2-benzylidene-N-(1-phenylethyl)hydrazinecarbothioamide (**3a**). Yellow crystals; yield 72%; mp. 88–89°C; [α]_D = –76.6 (c: 0.5, DMSO); UV (DMSO, λ_{\max} , nm): 334, 320, 258; IR (ν_{\max} , cm⁻¹): 3309 and 3187 (N-H), 1601 (C=N), 1205 (C=S); EI-MS (*m/z*): 283.1 [M]⁺; ¹H NMR (400 MHz, DMSO-*d*₆): δ 1.58 (d, 3H, *J* = 7.2 Hz, H-6'), 5.76 (p, 1H, H-1'), 7.25 (t, 1H, *J*₁, *J*₂ = 7.2 Hz, H-5'), 7.35 (t, 2H, *J*₁, *J*₂ = 7.6 Hz, H-4'), 7.43–7.45 (m, 5H, H-3', H-4'', H-5''), 7.84 (dd, 2H, *J*₁, *J*₂ = 7.2 Hz, H-3''), 8.12 (s, 1H, H-1''), 8.62 (d, 1H, *J* = 9.2 Hz, H-4), 11.58 (s, 1H, H-2); ¹³C NMR (100 MHz, DMSO-*d*₆): δ 21.77 (C-6'), 52.88 (C-1'), 126.79 (C-5'), 126.19 (C-3'), 127.89 (C-4'), 128.68 (C-4''), 129.13 (C-3''), 130.37 (C-5''), 134.53 (C-2''), 143.04 (C-2'), 144.30 (C=N, C-1''), 176.90 (C=S, C-3).

Chirality DOI 10.1002/chir

Anal. Calcd. for C₁₆H₁₇N₃S: C, 67.81; H, 6.05; N, 14.83; S, 11.31%. Found: C, 67.90; H, 6.03; N, 14.78; S, 11.32%.

(+)-(S)-2-benzylidene-N-(1-phenylethyl)hydrazinecarbothioamide (**3b**). Yellow crystals; yield 75%; mp. 92–93°C; [α]_D = +77.0 (c: 0.5, DMSO); UV (DMSO, λ_{\max} , nm): 334, 324, 256; IR (ν_{\max} , cm⁻¹): 3309 and 3183 (N-H), 1601 (C=N), 1203 (C=S); EI-MS (*m/z*): 283.1 [M]⁺; ¹H NMR (400 MHz, DMSO-*d*₆): δ 1.58 (d, 3H, *J* = 6.8 Hz, H-6'), 5.75 (p, 1H, H-1'), 7.25 (t, 1H, *J*₁, *J*₂ = 7.2 Hz, H-5'), 7.35 (t, 2H, *J*₁, *J*₂ = 7.6 Hz, H-4'), 7.42–7.45 (m, 5H, H-3', H-4'', H-5''), 7.83 (dd, 2H, *J*₁, *J*₂ = 7.2 Hz, H-3''), 8.11 (s, 1H, H-1''), 8.62 (d, 1H, *J* = 8.8 Hz, H-4), 11.58 (s, 1H, H-2); ¹³C NMR (100 MHz, DMSO-*d*₆): δ 21.76 (C-6'), 52.87 (C-1'), 126.79 (C-5'), 126.19 (C-3'), 127.89 (C-4'), 128.68 (C-4''), 129.13 (C-3''), 130.37 (C-5''), 134.53 (C-2''), 143.04 (C-2'), 144.30 (C=N, C-1''), 176.87 (C=S, C-3). Anal. Calcd. for C₁₆H₁₇N₃S: C, 67.81; H, 6.05; N, 14.83; S, 11.31%. Found: C, 67.92; H, 6.01; N, 14.75; S, 11.36%.

(–)-(R)-2-(4-bromobenzylidene)-N-(1-phenylethyl)hydrazinecarbothioamide (**4a**). Yellow crystals; yield 87%; mp. 153–154°C; [α]_D = –72.4 (c: 0.5, DMSO); UV (DMSO, λ_{\max} , nm): 340, 330, 260; IR (ν_{\max} , cm⁻¹): 3356 and 3141 (N-H), 1593 (C=N) 1209; (C=S); EI-MS (*m/z*): 363.2 [M+H]⁺; ¹H NMR (400 MHz, DMSO-*d*₆): δ 1.57 (d, 3H, *J* = 7.2 Hz, H-6'), 5.75 (p, 1H, H-1'), 7.25 (t, 1H, *J*₁, *J*₂ = 7.2 Hz, H-5'), 7.36 (t, 2H, *J*₁, *J*₂ = 7.6 Hz, H-4'), 7.42 (d, 2H, *J* = 8.8 Hz, H-3'), 7.62 (d, 2H, *J* = 8.4 Hz, H-4''), 7.80 (d, 2H, *J* = 8.4 Hz, H-3''), 8.07 (s, 1H, H-1''), 8.69 (d, 1H, *J* = 8.8 Hz, H-4), 11.61 (s, 1H, H-2); ¹³C NMR (100 MHz, DMSO-*d*₆): δ 21.71 (C-6'), 52.91 (C-1'), 123.57 (C-5'), 126.76 (C-5'), 127.18 (C-3'), 128.67 (C-4'), 129.78 (C-3''), 132.08 (C-4''), 133.85 (C-2''), 141.84 (C-2'), 144.22 (C=N, C-1''), 176.96 (C=S, C-3). Anal. Calcd. for C₁₆H₁₆BrN₃S: C, 53.04; H, 4.45; N, 11.60; S, 8.85%. Found: C, 53.06; H, 4.41; N, 11.76; S, 8.81%.

(+)-(S)-2-(4-bromobenzylidene)-N-(1-phenylethyl)hydrazinecarbothioamide (**4b**). Yellow crystals; yield 83%; mp. 154–155°C; [α]_D = +71.2 (c: 0.5, DMSO); UV (DMSO, λ_{\max} , nm): 339, 330, 259; IR (ν_{\max} , cm⁻¹): 3356 and 3145 (N-H), 1591 (C=N), 1208 (C=S); EI-MS (*m/z*): 363.1 [M+H]⁺; ¹H NMR (400 MHz, DMSO-*d*₆): δ 1.57 (d, 3H, *J* = 7.2 Hz, H-6'), 5.76 (p, 1H, H-1'), 7.25 (t, 1H, *J*₁, *J*₂ = 7.2 Hz, H-5'), 7.35 (t, 2H, *J*₁, *J*₂ = 7.6 Hz, H-4'), 7.42 (d, 2H, *J* = 8.8 Hz, H-3'), 7.62 (d, 2H, *J* = 8.4 Hz, H-4''), 7.81 (d, 2H, *J* = 8.4 Hz, H-3''), 8.07 (s, 1H, H-1''), 8.70 (d, 1H, *J* = 9.2 Hz, H-4), 11.62 (s, 1H, H-2); ¹³C NMR (100 MHz, DMSO-*d*₆): δ 21.72 (C-6'), 52.92 (C-1'), 123.57 (C-5'), 126.76 (C-5'), 127.18 (C-3'), 128.66 (C-4'), 129.77 (C-3''), 132.08 (C-4''), 133.86 (C-2''), 141.84 (C-2'), 144.22 (C=N, C-1''), 176.99 (C=S, C-3). Anal. Calcd. for C₁₆H₁₆BrN₃S: C, 53.04; H, 4.45; N, 11.60; S, 8.85%. Found: C, 53.08; H, 4.46; N, 11.72; S, 8.80%.

(–)-(R)-2-(4-chlorobenzylidene)-N-(1-phenylethyl)hydrazinecarbothioamide (**5a**). White crystals; yield 75%; mp. 138–139°C; [α]_D = –82.7 (c: 0.5, DMSO); UV (DMSO, λ_{\max} , nm): 339, 325, 259; IR (ν_{\max} , cm⁻¹): 3359 and 3142 (N-H), 1596 (C=N), 1205 (C=S); EI-MS (negative ion mode, *m/z*): 316.0 [M-H]⁺; ¹H NMR (400 MHz, DMSO-*d*₆): δ 1.57 (d, 3H, *J* = 7.2 Hz, H-6'), 5.75 (p, 1H, H-1'), 7.25 (t, 1H, *J*₁, *J*₂ = 7.2 Hz, H-5'), 7.35 (t, 2H, *J*₁, *J*₂ = 7.6 Hz, H-4'), 7.42 (d, 2H, *J* = 7.2 Hz, H-3'), 7.49 (d, 2H, *J* = 8.8 Hz, H-4''), 7.87 (d, 2H, *J* = 8.4 Hz, H-3''), 8.08 (s, 1H, H-1''), 8.69 (d, 1H, *J* = 8.8 Hz, H-4), 11.61 (s, 1H, H-2); ¹³C NMR 100 MHz, DMSO-*d*₆): δ 21.72 (C-6'),

52.90 (C-1'), 126.77 (C-5'), 127.17 (C-3'), 128.54 (C-4'), 130.50 (C-4''), 133.53 (C-3''), 134.75 (C-2''), 141.71 (C-5''), 143.99 (C-2'), 144.24 (C=N, C-1''), 176.97 (C=S, C-3). Anal. Calcd. for $C_{16}H_{16}ClN_3S$: C, 60.46; H, 5.07; N, 13.22; S, 10.09%. Found: C, 60.49; H, 5.06; N, 13.21; S, 10.10%.

(+)-(S)-2-(4-chlorobenzylidene)-N-(1-phenylethyl)hydrazinecarbothioamide (5b). White crystals; yield 81%; mp. 138–139°C; $[\alpha]_D = +81.2$ (c: 0.5, DMSO); UV (DMSO, λ_{max} , nm): 340, 330, 260; IR (ν_{max} , cm^{-1}): 3359 and 3139 (N-H), 1595 (C=N), 1205 (C=S); EI-MS (negative ion mode, m/z): 316.1 [M-H]⁺; ¹H NMR (400 MHz, DMSO-*d*₆): δ 1.57 (d, 3H, $J = 7.2$ Hz, H-6'), 5.76 (p, 1H, H-1'), 7.26 (t, 1H, $J_1, J_2 = 7.2$ Hz, H-5'), 7.36 (t, 2H, $J_1, J_2 = 7.6$ Hz, H-4'), 7.42 (d, 2H, $J = 7.2$ Hz, H-3'), 7.48 (d, 2H, $J = 8.8$ Hz, H-4''), 7.87 (d, 2H, $J = 8.4$ Hz, H-3''), 8.09 (s, 1H, H-1''), 8.71 (d, 1H, $J = 8.8$ Hz, H-4), 11.63 (s, 1H, H-2); ¹³C NMR (100 MHz, DMSO-*d*₆): δ 21.71 (C-6'), 52.89 (C-1'), 126.77 (C-5'), 127.17 (C-3'), 128.53 (C-4'), 130.51 (C-4''), 133.53 (C-3''), 134.76 (C-2''), 141.69 (C-5''), 143.96 (C-2'), 144.24 (C=N, C-1''), 176.96 (C=S, C-3). Anal. Calcd. for $C_{16}H_{16}ClN_3S$: C, 60.46; H, 5.07; N, 13.22; S, 10.09%. Found: C, 60.42; H, 5.09; N, 13.19; S, 10.05%.

(-)-(R)-2-(4-fluorobenzylidene)-N-(1-phenylethyl)hydrazinecarbothioamide (6a). White crystals; yield 71%; mp. 131–132°C; $[\alpha]_D = -84.0$ (c: 0.5, DMSO); UV (DMSO, λ_{max} , nm): 335, 320, 260; IR (ν_{max} , cm^{-1}): 3339 and 3172 (N-H), 1600 (C=N), 1204 (C=S); EI-MS (m/z): 301.2 [M]⁺; ¹H NMR (400 MHz, DMSO-*d*₆): δ 1.57 (d, 3H, $J = 6.8$ Hz, H-6'), 5.75 (p, 1H, H-1), 7.25 (t, 3H, $J_1, J_2 = 6.8$ Hz, H-5', H-3''), 7.35 (t, 2H, $J_1, J_2 = 7.6$ Hz, H-4'), 7.42 (d, 2H, $J = 7.2$ Hz, H-3'), 7.91 (dd, 2H, $J_1, J_2 = 8.8$ Hz, H-4''), 8.09 (s, 1H, H-1''), 8.67 (d, 1H, $J = 9.2$ Hz, H-4), 11.58 (s, 1H, H-2); ¹³C NMR (100 MHz, DMSO-*d*₆): δ 22.77 (C-6'), 52.89 (C-1'), 116.06 (C-4''), 126.75 (C-5'), 127.19 (C-3'), 128.68 (C-4'), 130.15 (C-2''), 131.14 (C-3''), 141.97 (C-2'), 144.26 (C=N, C-1''), 164.73 (C-5''), 176.89 (C=S, C-3). Anal. Calcd. for $C_{16}H_{16}FN_3S$: C, 63.43; H, 5.65; N, 13.93; S, 2.34%. Found: C, 63.56; H, 5.45; N, 13.84; S, 2.50%.

(+)-(S)-2-(4-fluorobenzylidene)-N-(1-phenylethyl)hydrazinecarbothioamide (6b). White crystals; yield 77%; mp. 134–135°C; $[\alpha]_D = +83.2$ (c: 0.5, DMSO); UV (DMSO, λ_{max} , nm): 335, 320, 260; IR (ν_{max} , cm^{-1}): 3339 and 3167 (N-H), 1601 (C=N), 1203 (C=S); EI-MS (m/z): 301.0 [M]⁺; ¹H NMR (400 MHz, DMSO-*d*₆): δ 1.57 (d, 3H, $J = 6.8$ Hz, H-6'), 5.75 (p, 1H, H-1), 7.25 (m, 3H, H-5', H-3''), 7.35 (t, 2H, $J_1, J_2 = 7.6$ Hz, H-4'), 7.42 (d, 2H, $J = 7.6$ Hz, H-3'), 7.91 (dd, 2H, $J_1, J_2 = 8.4$ Hz, H-4''), 8.10 (s, 1H, H-1''), 8.64 (d, 1H, $J = 8.8$ Hz, H-4), 11.56 (s, 1H, H-2); ¹³C NMR (100 MHz, DMSO-*d*₆): δ 22.77 (C-6'), 52.89 (C-1'), 116.07 (C-4''), 126.74 (C-5'), 127.19 (C-3'), 128.68 (C-4'), 130.16 (C-2''), 131.11 (C-3''), 141.96 (C-2'), 144.26 (C=N, C-1''), 164.72 (C-5''), 176.90 (C=S, C-3). Anal. Calcd. for $C_{16}H_{16}FN_3S$: C, 63.43; H, 5.65; N, 13.93; S, 2.34%. Found: C, 63.52; H, 5.49; N, 13.86; S, 2.42%.

(-)-(R)-2-(4-cyanobenzylidene)-N-(1-phenylethyl)hydrazinecarbothioamide (7a). Yellow crystals; yield 85%; mp. 167–168°C; $[\alpha]_D = -79.8$ (c: 0.5, DMSO); UV (DMSO, λ_{max} , nm): 359, 345, 259; IR (ν_{max} , cm^{-1}): 3369 and 3139 (N-H), 2224 (C≡N), 1596 (C=N), 1214 (C=S); EI-MS (negative ion mode, m/z): 307.0 [M-H]⁺; ¹H NMR (400 MHz, DMSO-*d*₆): δ 1.59 (d, 3H, $J = 7.2$ Hz, H-6'), 5.76 (p, 1H, H-1), 7.25 (t, 1H, $J_1, J_2 = 7.2$ Hz, H-5'), 7.35 (t, 2H, $J_1, J_2 = 7.6$ Hz, H-4'), 7.43 (d, 2H,

$J = 7.6$ Hz, H-3'), 7.87 (d, 2H, $J = 8.4$ Hz, H-4'), 8.04 (d, 2H, $J = 8.0$ Hz, H-3''), 8.14 (s, 1H, H-4''), 8.75 (d, 1H, $J = 8.8$ Hz, H-4), 11.73 (s, 1H, H-2). ¹³C NMR (100 MHz, DMSO-*d*₆): δ 21.66 (C-6'), 53.00 (C-1'), 112.01 (C-5''), 119.26 (C≡N), 126.76 (C-3''), 127.19 (C-5'), 128.67 (C-3'), 130.34 (C-4'), 133.66 (C-4''), 139.13 (C-2''), 140.91 (C-2'), 144.13 (C=N, C-1''), 177.19 (C=S, C-3). Anal. Calcd. for $C_{17}H_{16}N_4S$: C, 66.21; H, 5.23; N, 18.17; S, 10.40%. Found: C, 66.29; H, 5.17; N, 18.19; S, 10.52%.

(+)-(S)-2-(4-cyanobenzylidene)-N-(1-phenylethyl)hydrazinecarbothioamide (7b). Yellow crystals; yield 72%; mp. 166–167°C; $[\alpha]_D = +81.2$ (c: 0.5, DMSO); UV (DMSO, λ_{max} , nm): 360, 348; 260; IR (ν_{max} , cm^{-1}): 3370 and 3139 (N-H), 2224 (C≡N), 1595 (C=N), 1206 (C=S); EI-MS (negative ion mode, m/z): 307.0 [M-H]⁺; ¹H NMR (400 MHz, DMSO-*d*₆): δ 1.58 (d, 3H, $J = 7.2$ Hz, H-6'), 5.77 (p, 1H, H-1), 7.25 (t, 1H, $J_1, J_2 = 7.2$ Hz, H-5'), 7.35 (t, 2H, $J_1, J_2 = 7.6$ Hz, H-4'), 7.43 (d, 2H, $J = 7.6$ Hz, H-3'), 7.88 (d, 2H, $J = 8.0$ Hz, H-3''), 8.05 (d, 2H, $J = 7.6$ Hz, H-4''), 8.14 (s, 1H, H-1''), 8.76 (d, 1H, $J = 8.8$ Hz, H-4), 11.73 (s, 1H, H-2); ¹³C NMR (100 MHz, DMSO-*d*₆): δ 21.65 (C-6'), 53.00 (C-1'), 112.01 (C-5''), 119.28 (C≡N), 126.76 (C-3''), 127.19 (C-5'), 128.68 (C-3'), 130.34 (C-4'), 133.67 (C-4''), 139.13 (C-2''), 140.89 (C-2'), 144.13 (C=N, C-1''), 177.16 (C=S, C-3). Anal. Calcd. for $C_{17}H_{16}N_4S$: C, 66.21; H, 5.23; N, 18.17; S, 10.40%. Found: C, 66.31; H, 5.19; N, 18.22; S, 10.44%.

(-)-(R)-2-(4-hydroxybenzylidene)-N-(1-phenylethyl)hydrazinecarbothioamide (8a). Yellow crystals; yield 87%; mp. 171–172°C; $[\alpha]_D = -69.5$ (c: 0.5, DMSO); UV (DMSO, λ_{max} , nm): 344, 330, 304; IR (ν_{max} , cm^{-1}): 3359 and 3151 (N-H), 1605 (C=N), 1200 (C=S); EI-MS (m/z): 300.1 [M+H]⁺; ¹H NMR (400 MHz, DMSO-*d*₆): δ 1.56 (d, 3H, $J = 6.8$ Hz, H-6'), 5.73 (p, 1H, H-1), 6.81 (d, 2H, $J = 8.8$ Hz, H-4''), 7.26 (t, 1H, $J_1, J_2 = 7.2$ Hz, H-5'), 7.35 (t, 2H, $J_1, J_2 = 7.6$ Hz, H-4'), 7.42 (d, 2H, $J = 8.4$ Hz, H-3'), 7.65 (d, 2H, $J = 8.8$ Hz, H-3''), 8.01 (s, 1H, H-1''), 8.47 (d, 1H, $J = 9.2$ Hz, H-4), 9.94 (s, 1H, OH), 11.39 (s, 1H, H-2); ¹³C NMR (100 MHz, DMSO-*d*₆): δ 21.15 (C-6'), 52.03 (C-1'), 115.33 (C-4''), 124.75 (C-2''), 126.05 (C-5'), 126.46 (C-3'), 127.97 (C-4'), 128.95 (C-3''), 142.81 (C-2'), 143.69 (C=N, C-1''), 159.09 (C-5''); 175.74 (C=S, C-3). Anal. Calcd. for $C_{16}H_{17}N_3OS$: C, 64.19; H, 5.72; N, 14.04; S, 10.71%. Found: C, 64.28; H, 5.68; N, 14.19; S, 10.72%.

(+)-(S)-2-(4-hydroxybenzylidene)-N-(1-phenylethyl)hydrazinecarbothioamide (8b). Yellow crystals; yield 87%; mp. 173–174°C; $[\alpha]_D = +70.6$ (c: 0.5, DMSO); UV (DMSO, λ_{max} , nm): 344, 330, 305; IR (ν_{max} , cm^{-1}): 3360 and 3151 (N-H), 1605 (C=N), 1201 (C=S); EI-MS (m/z): 299.0 [M]⁺; ¹H NMR (400 MHz, DMSO-*d*₆): δ 1.56 (d, 3H, $J = 7.2$ Hz, H-6'), 5.73 (p, 1H, H-1), 6.82 (d, 2H, $J = 8.8$ Hz, H-4''), 7.26 (t, 1H, $J_1, J_2 = 7.2$ Hz, H-5'), 7.35 (t, 2H, $J_1, J_2 = 7.6$ Hz, H-4'), 7.42 (d, 2H, $J = 8.4$ Hz, H-3'), 7.65 (d, 2H, $J = 8.4$ Hz, H-3''), 8.01 (s, 1H, H-1''), 8.47 (d, 1H, $J = 9.2$ Hz, H-4), 9.96 (s, 1H, OH), 11.40 (s, 1H, H-2); ¹³C NMR (100 MHz, DMSO-*d*₆): δ 21.19 (C-6'), 52.02 (C-1'), 115.32 (C-4''), 124.76 (C-2''), 126.08 (C-5'), 126.48 (C-3'), 127.96 (C-4'), 128.97 (C-3''), 142.83 (C-2'), 143.68 (C=N, C-1''), 159.03 (C-5''); 175.71 (C=S, C-3). Anal. Calcd. for $C_{16}H_{17}N_3OS$: C, 64.19; H, 5.72; N, 14.04; S, 10.71%. Found: C, 64.16; H, 5.75; N, 14.11; S, 10.76%.

(-)-(R)-2-(4-methoxybenzylidene)-N-(1-phenylethyl)hydrazinecarbothioamide (9a). White crystals; yield 75%; mp. 143–144°C; $[\alpha]_D = -65.4$ (c: 0.5, DMSO); UV (DMSO, λ_{max} , nm): 345, 330, 260; IR (ν_{max} , cm^{-1}): 3361 and 3149 (N-H), 1605 (C=N), 1201

(C=S); EI-MS (m/z): 313.1 [M]⁺; ¹H NMR (400 MHz, DMSO-*d*₆): δ 1.57 (d, 3H, J =6.8 Hz, H-6'), 3.80 (s, 3H, OCH₃, H-6''), 5.74 (p, 1H, H-1), 6.99 (d, 2H, J =8.8 Hz, H-4''), 7.25 (t, 1H, J_1, J_2 =7.2 Hz, H-5'), 7.35 (t, 2H, J_1, J_2 =7.6 Hz, H-4'), 7.43 (d, 2H, J =8.0 Hz, H-3'), 7.77 (d, 2H, J =8.8 Hz, H-3''), 8.05 (s, 1H, H-1''), 8.54 (d, 1H, J =9.2 Hz, H-4), 11.46 (s, 1H, H-2); ¹³C NMR (100 MHz, DMSO-*d*₆): δ 21.83 (C-6'), 52.79 (C-1'), 55.74 (–OCH₃, C-6''), 114.62 (C-4''), 126.77 (C-2''), 127.07 (C-5'), 127.17 (C-3'), 128.67 (C-4'), 129.53 (C-3''), 143.03 (C-2'), 144.37 (C=N, C-1''), 161.20 (C-5''), 176.58 (C=S, C-3). Anal. Calcd. for C₁₇H₁₉N₃OS: 65.15; H, 6.11; N, 13.41; S, 10.23%. Found: C, 65.22; H, 6.16; N, 13.45; S, 10.27%.

(+)-(S)-2-(4-methoxybenzylidene)-N-(1-phenylethyl)hydrazinecarbothioamide (9b). White crystals; yield 77%; mp. 145–146 °C; [α]_D = +64.8 (c: 0.5, DMSO); UV (DMSO, λ_{max}, nm): 345, 330, 262; IR (ν_{max}, cm⁻¹): 3361 and 3149 (N-H), 1609 (C=N) 1200 (C=S); EI-MS (m/z): 313.0 [M]⁺; ¹H NMR (400 MHz, DMSO-*d*₆): δ 1.57 (d, 3H, J =6.8 Hz, H-6'), 3.81 (s, 3H, OCH₃, H-6''), 5.74 (p, 1H, H-1), 6.99 (d, 2H, J =8.8 Hz, H-4''), 7.25 (t, 1H, J_1, J_2 =7.2 Hz, H-5'), 7.35 (t, 2H, J_1, J_2 =7.6 Hz, H-4'), 7.43 (d, 2H, J =8.0 Hz, H-3'), 7.77 (d, 2H, J =8.8 Hz, H-3''), 8.06 (s, 1H, H-1''), 8.54 (d, 1H, J =8.8 Hz, H-4), 11.46 (s, 1H, H-2); ¹³C NMR (100 MHz, DMSO-*d*₆): δ 21.84 (C-6'), 52.75 (C-1'), 55.80 (–OCH₃, C-6''), 114.63 (C-4''), 126.77 (C-2''), 127.08 (C-5'), 127.17 (C-3'), 128.67 (C-4'), 129.52 (C-3''), 143.08 (C-2'), 144.36 (C=N, C-1''), 161.21 (C-5''), 176.61 (C=S, C-3). Anal. Calcd. for C₁₇H₁₉N₃OS: 65.15; H, 6.11; N, 13.41; S, 10.23%. Found: C, 65.12; H, 6.08; N, 13.51; S, 10.19%.

(–)-(R)-2-[4-(4-chlorophenoxy)benzylidene]-N-(1-phenylethyl)hydrazinecarbothioamide (10a). Yellow crystals; yield 70%; mp. 136–137 °C; [α]_D = –53.8 (c: 0.5, DMSO); UV (DMSO, λ_{max}, nm): 344, 330, 259; IR (ν_{max}, cm⁻¹): 3350 and 3155 (N-H), 1602 (C=N), 1207 (C=S); EI-MS (m/z): 409.1 [M]⁺; ¹H NMR (400 MHz, DMSO-*d*₆): δ 1.57 (d, 3H, J =6.8 Hz, H-6'), 5.75 (p, 1H, H-1), 7.01 (d, 2H, J =8.8 Hz, H-4''), 7.19 (m, 2H, H-9''), 7.24 (t, 3H, J_1, J_2 =7.2 Hz, H-5', H-8''), 7.34 (t, 2H, J_1, J_2 =7.6 Hz, H-4'), 7.43 (d, 2H, J =8.0 Hz, H-3'), 7.84 (d, 2H, J_1, J_2 =8.4 Hz, H-3''), 8.10 (s, 1H, H-1''), 8.52 (d, 1H, J =8.8 Hz, H-4), 11.50 (s, 1H, H-2); ¹³C NMR (100 MHz, DMSO-*d*₆): δ 21.81 (C-6'), 52.84 (C-1'), 118.23 (C-4''), 122.13 (C-8''), 126.77 (C-2''), 127.18 (C-5'), 127.58 (C-10''), 128.68 (C-3'), 129.87 (C-4'), 130.81 (C-9''), 132.48 (C-3''), 142.29 (C-2'), 144.31 (C=N, C-1''), 157.82 (C-7''), 161.01 (C-5''), 176.78 (C=S, C-3). Anal. Calcd. for C₂₂H₂₀ClN₃OS: 64.46; H, 4.92; N, 10.25; S, 7.82%. Found: C, 64.49; H, 4.98; N, 10.21; S, 7.76%.

(+)-(S)-2-[4-(4-chlorophenoxy)benzylidene]-N-(1-phenylethyl)hydrazinecarbothioamide (10b). Yellow crystals; yield 85%; mp. 138–139 °C; [α]_D = +52.7 (c: 0.5, DMSO); UV (DMSO, λ_{max}, nm): 344, 330, 259; IR (ν_{max}, cm⁻¹): 3350 and 3157 (N-H), 1605 (C=N), 1207 (C=S); EI-MS (m/z): 409.1 [M]⁺; ¹H NMR (400 MHz, DMSO-*d*₆): δ 1.57 (d, 3H, J =6.8 Hz, H-6'), 5.75 (p, 1H, H-1), 7.01 (d, 2H, J =8.8 Hz, H-4''), 7.15 (m, 2H, H-9''), 7.24 (t, 3H, J_1, J_2 =7.2 Hz, H-5', H-8''), 7.35 (t, 2H, J_1, J_2 =7.6 Hz, H-4'), 7.43 (d, 2H, J =8.4 Hz, H-3'), 7.84 (d, 2H, J =8.4 Hz, H-3''), 8.09 (s, 1H, H-1''), 8.53 (d, 1H, J =8.8 Hz, H-4), 11.50 (s, 1H, H-2); ¹³C NMR (100 MHz, DMSO-*d*₆): δ 21.81 (C-6'), 52.84 (C-1'), 118.23 (C-4''), 122.13 (C-8''), 126.77 (C-2''), 127.18 (C-5'), 128.67 (C-3'), 127.58 (C-10''), 129.86 (C-4'), 130.81 (C-9''), 132.48 (C-3''), 142.29 (C-2'), 144.31 (C=N, C-1''), 157.82 (C-7''), 161.03 (C-5''), 176.80 (C=S, C-3). Anal. Calcd. for C₂₂H₂₀ClN₃OS: 64.46; H, 4.92; N, 10.25; S, 7.82%. Found: C, 64.49; H, 4.98; N, 10.21; S, 7.76%.

Chirality DOI 10.1002/chir

64.46; H, 4.92; N, 10.25; S, 7.82%. Found: C, 64.52; H, 4.87; N, 10.20; S, 7.88%.

(R)-(–)-2-[4-(4-fluorophenoxy)benzylidene]-N-(1-phenylethyl)hydrazinecarbothioamide (11a). Yellow crystals; yield 74%; mp. 99–100 °C; [α]_D = –71.8 (c: 0.5, DMSO); UV (DMSO, λ_{max}, nm): 344, 330, 259; IR (ν_{max}, cm⁻¹): 3356 and 3158 (N-H), 1601 (C=N), 1237 (C=S); EI-MS (m/z): 393.2 [M]⁺; ¹H NMR (400 MHz, DMSO-*d*₆): δ 1.57 (d, 3H, J =7.2 Hz, H-6'), 5.75 (p, 1H, H-1), 7.11 (dd, 4H, J_1, J_2 =8.8 Hz, H-8'', H-9''), 7.25 (t, 1H, J_1, J_2 =7.2 Hz, H-5'), 7.35 (t, 2H, J_1, J_2 =7.6 Hz, H-4'), 7.43 (d, 2H, J =7.6 Hz, H-3'), 7.46 (d, 2H, J =8.8 Hz, H-3''), 7.86 (d, 2H, J =8.8 Hz, H-4''), 8.11 (s, 1H, H-1''), 8.55 (d, 1H, J =8.8 Hz, H-4), 11.51 (s, 1H, H-2); ¹³C NMR (100 MHz, DMSO-*d*₆): δ 21.82 (C-6'), 52.83 (C-1'), 118.23 (C-9''), 119.02 (C-4''), 126.77 (C-2''), 127.18 (C-5'), 128.22 (C-3'), 129.86 (C-4'), 132.50 (C-3''), 142.29 (C-2'), 144.31 (C=N, C-1''), 153.26 (C-7''), 155.44 (C-10''), 158.23 (C-5''), 176.80 (C=S, C-3). Anal. Calcd. for C₂₂H₂₀FN₃OS: 67.15; H, 5.12; N, 10.68; S, 8.15%. Found: C, 67.19; H, 5.12; N, 10.76; S, 8.10%.

(+)-(S)-2-[4-(4-fluorophenoxy)benzylidene]-N-(1-phenylethyl)hydrazinecarbothioamide (11b). Yellow crystals; yield 87%; mp. 101–102 °C; [α]_D = +72.6 (c: 0.5, DMSO); UV (DMSO, λ_{max}, nm): 344, 330, 259; IR (ν_{max}, cm⁻¹): 3350 and 3156 (N-H), 1604 (C=N), 1236 (C=S); EI-MS (m/z): 393.2 [M]⁺; ¹H NMR (400 MHz, DMSO-*d*₆): δ 1.57 (d, 3H, J =7.2 Hz, H-6'), 5.75 (p, 1H, H-1), 7.11 (dd, 4H, J_1, J_2 =8.8 Hz, H-8'', H-9''), 7.25 (t, 1H, J_1, J_2 =7.2 Hz, H-5'), 7.35 (t, 2H, J_1, J_2 =7.6 Hz, H-4'), 7.43 (d, 2H, J =7.6 Hz, H-3'), 7.46 (d, 2H, J =8.8 Hz, H-3''), 7.87 (d, 2H, J =8.8 Hz, H-4''), 8.10 (s, 1H, H-1''), 8.58 (d, 1H, J =8.8 Hz, H-4), 11.53 (s, 1H, H-2); ¹³C NMR (100 MHz, DMSO-*d*₆): δ 21.81 (C-6'), 52.84 (C-1'), 118.23 (C-9''), 119.02 (C-4''), 126.77 (C-2''), 127.18 (C-5'), 128.25 (C-3'), 129.87 (C-4'), 132.51 (C-3''), 142.29 (C-2'), 144.31 (C=N, C-1''), 153.26 (C-7''), 155.44 (C-10''), 158.23 (C-5''), 176.79 (C=S, C-3). Anal. Calcd. for C₂₂H₂₀FN₃OS: 67.15; H, 5.12; N, 10.68; S, 8.15%. Found: C, 67.20; H, 5.16; N, 10.61; S, 8.22%.

(–)-(R)-2-(4-methylthiobenzylidene)-N-(1-phenylethyl)hydrazinecarbothioamide (12a). Yellow crystals; yield 77%; mp. 106–107 °C; [α]_D = –84.8 (c: 0.5, DMSO); UV (DMSO, λ_{max}, nm): 360, 345, 259; IR (ν_{max}, cm⁻¹): 3350 and 3153 (N-H), 1593 (C=N), (C=S) 1238; EI-MS (m/z): 329.6 [M]⁺; ¹H NMR (400 MHz, DMSO-*d*₆): δ 1.57 (d, 3H, J =6.8 Hz, H-6'), 2.53 (s, 3H, SCH₃, H-6''), 5.76 (p, 1H, H-1), 7.25 (t, 1H, J_1 =8.0 Hz, J_2 =7.2 Hz, H-5'), 7.28 (d, 2H, J =8.0 Hz, H-4''), 7.35 (t, 2H, J_1 =7.2 Hz, J_2 =7.6 Hz, H-4'), 7.43 (d, 2H, J =8.0 Hz, H-3'), 7.81 (d, 2H, J =8.4 Hz, H-3''), 8.06 (s, 1H, H-1''), 8.62 (d, 1H, J =8.8 Hz, H-4), 11.53 (s, 1H, H-4); ¹³C NMR (100 MHz, DMSO-*d*₆): δ 14.76 (SCH₃, C-6''), 21.79 (C-6'), 52.85 (C-1'), 125.95 (C-5'), 126.78 (C-3'), 127.18 (C-4''), 128.48 (C-4'), 129.16 (C-3''), 130.99 (C-2''), 141.21 (C-2'), 142.68 (C-5''), 144.32 (C=N, C-1''), 176.73 (C=S, C-3). Anal. Calcd. for C₁₇H₁₉N₃S₂: C, 61.97; H, 5.81; N, 12.75; S, 19.46%. Found: C, 61.85; H, 5.83; N, 12.61; S, 19.36%.

(+)-(S)-2-(4-methylthiobenzylidene)-N-(1-phenylethyl)hydrazinecarbothioamide (12b). Yellow crystals; yield 81%; mp. 109–110 °C; [α]_D = +83.2 (c: 0.5, DMSO); UV (DMSO, λ_{max}, nm): 360, 345, 259; IR (ν_{max}, cm⁻¹): 3350 and 3151 (N-H), 1593 (C=N), 1238 (C=S); EI-MS (m/z): 330.1 [M+H]⁺; ¹H NMR (400 MHz, DMSO-*d*₆): δ 1.57 (d, 3H, J =6.8 Hz, H-6'), 2.52 (s, 3H, H-6''), 5.76 (p, 1H, H-1), 7.24 (t, 1H, J_1 =8.0 Hz, J_2 =7.2 Hz, H-5'), 7.29 (d, 2H, J =8.0 Hz,

H-4^{''}), 7.35 (t, 2H, $J_1=7.2$ Hz, $J_2=7.6$ Hz, H-4'), 7.43 (d, 2H, $J=8.0$ Hz, H-3'), 7.80 (d, 2H, $J=8.0$ Hz, H-3''), 8.05 (s, 1H, H-1''), 8.60 (d, 1H, $J=8.8$ Hz, H-4), 11.54 (s, 1H, H-2); ¹³C NMR (100 MHz, DMSO-*d*₆): δ 14.76 (SCH₃, C-6''), 21.79 (C-6'), 52.85 (C-1'), 125.97 (C-5'), 126.78 (C-3'), 127.18 (C-4''), 128.41 (C-4'), 129.16 (C-3''), 130.99 (C-2''), 141.20 (C-2'), 142.68 (C-5''), 144.31 (C=N, C-1''), 176.74 (C=S, C-3). Anal. Calcd. for C₁₇H₁₉N₃S₂: C, 61.97; H, 5.81; N, 12.75; S, 19.46%. Found: C, 61.92; H, 5.76; N, 12.80; S, 19.51%.

(-)-(R)-2-(4-trifluoromethylthiobenzylidene)-N-(1-phenylethyl)hydrazinocarbothioamide (13a). White crystals; yield 76%; mp. 146–147°C; [α]_D = -72.4 (c: 0.5, DMSO); UV (DMSO, λ_{max}, nm): 335, 260; IR (ν_{max}, cm⁻¹): 3360 and 3141 (N-H), 1600 (C=N), 1235 (C=S); EI-MS (negative ion mode, *m/z*): 382.0 [M-H]⁺; ¹H NMR (400 MHz, DMSO-*d*₆): δ 1.58 (d, 3H, $J=6.8$ Hz, H-6'), 5.75 (p, 1H, H-1), 7.25 (t, 1H, $J_1, J_2=7.6$ Hz, H-5'), 7.35 (t, 2H, $J_1, J_2=7.6$ Hz, H-4'), 7.43 (d, 2H, $J=7.2$ Hz, H-3'), 7.75 (d, 2H, $J=8.0$ Hz, H-4''), 7.99 (d, 2H, $J=8.4$ Hz, H-3''), 8.14 (s, 1H, H-1''), 8.71 (d, 1H, $J=8.8$ Hz, H-4), 11.69 (s, 1H, H-2); ¹³C NMR (100 MHz, DMSO-*d*₆): δ 21.71 (C-6'), 52.95 (C-1'), 126.76 (C-5'), 127.19 (C-4''), 128.46 (C-3'), 129.04 (C-4'), 131.52 (C-3''), 134.62 (C-2''), 136.73 (SCF₃, C-6''), 137.56 (C-5''), 141.23 (C-2'), 144.18 (C=N, C-1''), 177.08 (C=S, C-3). Anal. Calcd. for C₁₇H₁₆F₃N₃S₂: C, 53.25; H, 4.21; N, 10.96; S, 16.72%. Found: C, 53.16; H, 4.31; N, 11.09; S, 16.68%.

(+)-(S)-2-(4-trifluoromethylthiobenzylidene)-N-(1-phenylethyl)hydrazinocarbothioamide (13b). Yellow crystals; yield 80%; mp. 150–151°C; [α]_D = +71.9 (c: 0.5, DMSO); UV (DMSO, λ_{max}, nm): 340, 260; IR (ν_{max}, cm⁻¹): 3360 and 3141 (N-H), 1600 (C=N), 1235 (C=S); EI-MS (negative ion mode, *m/z*): 382.1 [M-H]⁺; ¹H NMR (400 MHz, DMSO-*d*₆): δ 1.58 (d, 3H, $J=7.2$ Hz, H-6'), 5.75 (p, 1H, H-1), 7.25 (t, 1H, $J_1, J_2=7.6$ Hz, H-5'), 7.35 (t, 2H, $J_1, J_2=7.6$ Hz, H-4'), 7.43 (d, 2H, $J=7.6$ Hz, H-3'), 7.75 (d, 2H, $J=8.4$ Hz, H-4''), 7.99 (d, 2H, $J=8.4$ Hz, H-3''), 8.14 (s, 1H, H-1''), 8.74 (d, 1H, $J=8.8$ Hz, H-4), 11.70 (s, 1H, H-2); ¹³C NMR (100 MHz, DMSO-*d*₆): δ 21.75 (C-6'), 52.95 (C-1'), 126.75 (C-5'), 127.19 (C-4''), 128.45 (C-3'), 129.03 (C-4'), 131.52 (C-3''), 134.61 (C-2''), 136.72 (SCF₃, C-6''), 137.56 (C-5''), 141.21 (C-2'), 144.18 (C=N, C-1''), 177.09 (C=S, C-3). Anal. Calcd. for C₁₇H₁₆F₃N₃S₂: C, 53.25; H, 4.21; N, 10.96; S, 16.72%. Found: C, 53.32; H, 4.18; N, 10.89; S, 16.74%.

(-)-(R)-2-(4-nitrobenzylidene)-N-(1-phenylethyl)hydrazinocarbothioamide (14a). Yellow crystals; yield 84%; mp. 170–171°C; [α]_D = -42.8 (c: 0.5, DMSO); UV (DMSO, λ_{max}, nm): 380, 265, 254; IR (ν_{max}, cm⁻¹): 3355 and 3107 (N-H), 1599 (C=N), 1205 (C=S); EI-MS (negative ion mode, *m/z*): 327.0 [M-H]⁺; ¹H NMR (400 MHz, DMSO-*d*₆): δ 1.59 (d, 3H, $J=7.2$ Hz, H-6'), 5.77 (p, 1H, H-1), 7.25 (t, 1H, $J_1, J_2=7.2$ Hz, H-5'), 7.36 (t, 2H, $J_1, J_2=7.6$ Hz, H-4'), 7.43 (d, 2H, $J=8.0$ Hz, H-3'), 8.12 (d, 2H, $J=8.8$ Hz, H-4''), 8.19 (s, 1H, H-1''), 8.25 (d, 2H, $J=8.4$ Hz, H-3''), 8.89 (d, 1H, $J=8.8$ Hz, H-4), 11.86 (s, 1H, H-2); ¹³C NMR (100 MHz, DMSO-*d*₆): δ 21.64 (C-6'), 53.04 (C-1'), 124.25 (C-4''), 126.76 (C-3''), 127.21 (C-5'), 128.68 (C-3'), 129.16 (C-4'), 140.44 (C-2''), 141.03 (C-2'), 144.07 (C=N, C-1''), 148.05 (C-5''), 177.22 (C=S, C-3). Anal. Calcd. for C₁₆H₁₆N₄O₂S₂: C, 58.52; H, 4.91; N, 17.06; S, 9.76%. Found: C, 58.49; H, 4.86; N, 17.11; S, 9.66%.

(+)-(S)-2-(4-nitrobenzylidene)-N-(1-phenylethyl)hydrazinocarbothioamide (14b). Yellow crystals; yield 74%; mp. 167–168°C; [α]_D = +43.7 (c: 0.5, DMSO); UV (DMSO, λ_{max}, nm): 370,

265, 255; IR (ν_{max}, cm⁻¹): 3339 and 3167 (N-H), 1600 (C=N), 1205 (C=S); EI-MS (negative ion mode, *m/z*): 327.1 [M-H]⁺; ¹H NMR (400 MHz, DMSO-*d*₆): δ 1.59 (d, 3H, $J=6.8$ Hz, H-6'), 5.77 (p, 1H, H-1), 7.25 (t, 1H, $J_1, J_2=7.2$ Hz, H-5'), 7.35 (t, 2H, $J_1, J_2=7.6$ Hz, H-4'), 7.42 (d, 2H, $J=7.6$ Hz, H-3'), 8.12 (d, 2H, $J=8.0$ Hz, H-4''), 8.18 (s, 1H, H-1''), 8.26 (d, 2H, $J=8.4$ Hz, H-3''), 8.88 (d, 1H, $J=8.8$ Hz, H-4), 11.84 (s, 1H, H-2); ¹³C NMR (100 MHz, DMSO-*d*₆): δ 21.64 (C-6'), 53.04 (C-1'), 124.25 (C-4''), 126.76 (C-3''), 127.21 (C-5'), 128.68 (C-3'), 129.18 (C-4'), 140.44 (C-2''), 141.04 (C-2'), 144.09 (C=N, C-1''), 148.06 (C-5''), 177.21 (C=S, C-3). Anal. Calcd. for C₁₆H₁₆N₄O₂S₂: C, 58.52; H, 4.91; N, 17.06; S, 9.76%. Found: C, 58.56; H, 4.87; N, 17.04; S, 9.69%.

(-)-(R)-2-[(4-pyrrolidin-1-yl)benzylidene]-N-(1-phenylethyl)hydrazinocarbothioamide (15a). Brown crystals; yield 77%; mp. 142–143°C; [α]_D = -105.4 (c: 0.5, DMSO); UV (DMSO, λ_{max}, nm): 365, 339, 260; IR (ν_{max}, cm⁻¹): 3361 and 3124 (N-H), 1597 (C=N), 1200 (C=S); EI-MS (*m/z*): 352.8 [M]⁺; ¹H NMR (400 MHz, DMSO-*d*₆): δ 1.57 (d, 3H, $J=6.8$ Hz, H-6'), 1.96 (s, 4H, CH₂, H-7''), 3.28 (s, 4H, NCH₂, H-6''), 5.72 (p, 1H, H-1), 6.56 (d, 2H, $J=8.8$ Hz, H-4''), 7.25 (t, 1H, $J_1, J_2=7.2$ Hz, H-5'), 7.35 (t, 2H, $J_1, J_2=7.6$ Hz, H-4'), 7.43 (d, 2H, $J=7.6$ Hz, H-3'), 7.58 (d, 2H, $J=8.4$ Hz, H-3''), 7.99 (s, 1H, H-1''), 8.34 (d, 1H, $J=8.8$ Hz, H-4), 11.27 (s, 1H, H-2); ¹³C NMR (100 MHz, DMSO-*d*₆): δ 22.60 (C-6'), 26.05 (NCH₂, C-6''), 48.34 (CH₂, C-7''), 53.31 (C-1'), 112.55 (C-4''), 121.68 (C-2''), 126.81 (C-5'), 127.81 (C-3'), 129.33 (C-4'), 130.00 (C-3''), 144.50 (C=N, C-1''), 145.12 (C-2'), 149.93 (C-5''), 176.64 (C=S, C-3). Anal. Calcd. for C₂₀H₂₄N₄S: C, 68.15; H, 6.86; N, 15.89; S, 9.10%. Found: C, 68.16; H, 6.95; N, 15.77; S, 9.19%.

(+)-(S)-2-[(4-pyrrolidin-1-yl)benzylidene]-N-(1-phenylethyl)hydrazinocarbothioamide (15b). Brown crystals; yield 78%; mp. 140–141°C; [α]_D = +104.4 (c: 0.5, DMSO); UV (DMSO, λ_{max}, nm): 365, 339, 259; IR (ν_{max}, cm⁻¹): 3357 and 3131 (N-H), 1599 (C=N), 1200 (C=S); EI-MS (*m/z*): 352.8 [M]⁺; ¹H NMR (400 MHz, DMSO-*d*₆): δ 1.56 (d, 3H, $J=6.8$ Hz, H-6'), 1.96 (s, 4H, CH₂, H-7''), 3.26 (s, 4H, NCH₂, H-6''), 5.71 (p, 1H, H-1), 6.55 (d, 2H, $J=8.8$ Hz, H-4''), 7.25 (t, 1H, $J_1, J_2=7.2$ Hz, H-5'), 7.35 (t, 2H, $J_1, J_2=7.6$ Hz, H-4'), 7.42 (d, 2H, $J=7.6$ Hz, H-3'), 7.58 (d, 2H, $J=8.4$ Hz, H-3''), 7.98 (s, 1H, H-1''), 8.33 (d, 1H, $J=8.8$ Hz, H-4), 11.28 (s, 1H, H-2); ¹³C NMR (100 MHz, DMSO-*d*₆): δ 22.61 (C-6'), 26.06 (NCH₂, C-6''), 48.33 (CH₂, C-7''), 53.30 (C-1'), 112.53 (C-4''), 121.63 (C-2''), 126.80 (C-5'), 127.82 (C-3'), 129.37 (C-4'), 130.01 (C-3''), 144.49 (C=N, C-1''), 145.12 (C-2'), 149.92 (C-5''), 176.62 (C=S, C-3). Anal. Calcd. for C₂₀H₂₄N₄S: C, 68.15; H, 6.86; N, 15.89; S, 9.10%. Found: C, 68.21; H, 6.87; N, 15.82; S, 9.12%.

(-)-(R)-2-[(4-morpholin-4-yl)benzylidene]-N-(1-phenylethyl)hydrazinocarbothioamide (16a). Yellow crystals; yield 69%; mp. 98–99°C; [α]_D = -94.0 (c: 0.5, DMSO); UV (DMSO, λ_{max}, nm): 360, 349, 259; IR (ν_{max}, cm⁻¹): 3348 and 3143 (N-H), 1599 (C=N), 1225 (C=S); EI-MS (negative ion mode, *m/z*): 367.2 [M-H]⁺; ¹H NMR (400 MHz, DMSO-*d*₆): δ 1.57 (d, 3H, $J=7.2$ Hz, H-6'), 3.21 (t, 4H, $J_1, J_2=4.8$ Hz, NCH₂, H-7''), 3.74 (t, 4H, $J_1, J_2=5.2$ Hz, OCH₂, H-6''), 5.74 (p, 1H, H-1), 6.96 (d, 2H, $J=8.8$ Hz, H-4''), 7.25 (t, 1H, $J_1, J_2=7.2$ Hz, H-5'), 7.35 (t, 2H, $J_1, J_2=7.6$ Hz, H-4'), 7.43 (d, 2H, $J=7.6$ Hz, H-3'), 7.67 (d, 2H, $J=8.8$ Hz, H-3''), 8.01 (s, 1H, H-1''), 8.46 (d, 1H, $J=9.2$ Hz, H-4), 11.38 (s, 1H, H-2); ¹³C NMR (100 MHz, DMSO-*d*₆): δ 21.88 (C-6'), 47.95 (NCH₂, C-6''), 52.75 (C-1'), 66.41 (OCH₂, C-7''), 114.72 (C-4''), 124.73 (C-2''), 126.78 (C-5'), 127.17 (C-3'), 128.68 (C-4'), 129.09 (C-3''), 143.50

(C-2'), 144.42 (C=N, C-1''), 152.60 (C-5''), 176.36 (C=S, C-3). Anal. Calcd. for C₂₀H₂₄N₄OS: C, 65.19; H, 6.56; N, 15.20; S, 8.70%. Found: C, 65.09; H, 6.50; N, 15.33; S, 8.76%.

(+)-(S)-2-[(4-morpholin-4-yl)benzylidene]-N-(1-phenylethyl)hydrazine carbothioamide (16b). Yellow crystals; yield 80%; mp. 96–97°C; [α]_D = +95.6 (c: 0.5, DMSO); UV (DMSO, λ_{max}, nm): 360, 349, 259; IR (ν_{max}, cm⁻¹): 3348 and 3136 (N-H), 1600 (C=N), 1226 (C=S); EI-MS (negative ion mode, *m/z*): 367.0 [M-H]⁺; ¹H NMR (400 MHz, DMSO-*d*₆): δ 1.56 (d, 3H, *J* = 6.8 Hz, H-6'), 3.21 (t, 4H, *J*₁, *J*₂ = 4.8 Hz, NCH₂, H-7''), 3.74 (t, 4H, *J*₁ = 4.4 Hz, *J*₂ = 5.2 Hz, OCH₂, H-6''), 5.74 (p, 1H, H-1), 6.97 (d, 2H, *J* = 8.8 Hz, H-4''), 7.24 (t, 1H, *J*₁, *J*₂ = 7.2 Hz, H-5'), 7.35 (t, 2H, *J*₁, *J*₂ = 7.6 Hz, H-4'), 7.43 (d, 2H, *J* = 7.6 Hz, H-3'), 7.67 (d, 2H, *J* = 8.8 Hz, H-3''), 8.01 (s, 1H, H-1''), 8.46 (d, 1H, *J* = 8.8 Hz, H-4), 11.38 (s, 1H, H-2); ¹³C NMR (100 MHz, DMSO-*d*₆): δ 21.88 (C-6'), 47.94 (NCH₂, C-6''), 52.75 (C-1'), 66.40 (OCH₂, C-7''), 114.72 (C-4''), 124.73 (C-2''), 126.78 (C-5'), 127.16 (C-3'), 128.67 (C-4'), 129.08 (C-3''), 143.50 (C-2'), 144.42 (C=N, C-1''), 152.59 (C-5''), 176.34 (C=S, C-3). Anal. Calcd. for C₂₀H₂₄N₄OS: C, 65.19; H, 6.56; N, 15.20; S, 8.70%. Found: C, 65.23; H, 6.51; N, 15.28; S, 8.79%.

(-)-(R)-2-[(4-piperidin-1-yl)benzylidene]-N-(1-phenylethyl)hydrazinecarbothioamide (17a). Yellow crystals; yield 69%; mp. 80–81°C; [α]_D = -67.3 (c: 0.5, DMSO); UV (DMSO, λ_{max}, nm): 365, 355, 259; IR (ν_{max}, cm⁻¹): 3371 and 3196 (N-H), 1599 (C=N), 1221 (C=S); EI-MS (negative ion mode, *m/z*): 365.0 [M-H]⁺; ¹H NMR (400 MHz, DMSO-*d*₆): δ 1.56 (d, 3H, *J* = 7.2 Hz, H-6'), 1.57 (brs, 6H, CH₂CH₂, H-7'', H-8'') 3.25 (t, 4H, *J*₁, *J*₂ = 5.2 Hz, NCH₂, H-6''), 5.73 (p, 1H, H-1), 6.93 (d, 2H, *J* = 8.8 Hz, H-4''), 7.25 (t, 1H, *J*₁, *J*₂ = 6.8 Hz, *J*₂ = 7.6 Hz, H-5'), 7.35 (t, 2H, *J*₁, *J*₂ = 7.6 Hz, H-4'), 7.43 (d, 2H, *J* = 7.6 Hz, H-3'), 7.62 (d, 2H, *J* = 8.8 Hz, H-3''), 7.99 (s, 1H, H-1''), 8.42 (d, 1H, *J* = 9.2 Hz, H-4), 11.35 (s, 1H, H-2); ¹³C NMR (100 MHz, DMSO-*d*₆): δ 21.96 (C-6'), 24.39 (CH₂, C-8''), 25.02 (CH₂, C-7''), 48.17 (NCH₂, C-6'') 52.72 (C-1'), 113.60 (C-4''), 123.53 (C-2''), 126.76 (C-5'), 127.15 (C-3'), 128.70 (C-4'), 129.18 (C-3''), 143.68 (C-2'), 144.48 (C=N, C-1''), 152.72 (C-5''), 176.20 (C=S, C-3). Anal. Calcd. for C₂₁H₂₆N₄S: C, 68.82; H, 7.15; N, 15.29; S, 8.75%. Found: C, 68.79; H, 7.12; N, 15.33; S, 8.88%.

(+)-(S)-2-[(4-piperidin-1-yl)benzylidene]-N-(1-phenylethyl)hydrazinecarbothioamide (17b). Yellow crystals; yield 72%; mp. 79–80°C; [α]_D = +66.8 (c: 0.5, DMSO); UV (DMSO, λ_{max}, nm): 364, 355, 260; IR (ν_{max}, cm⁻¹): 3372 and 3195 (N-H), 1599 (C=N), 1222 (C=S); EI-MS (negative ion mode, *m/z*): 364.8 [M-H]⁺; ¹H NMR (400 MHz, DMSO-*d*₆): δ 1.56 (d, 3H, *J* = 7.2 Hz, H-6'), 1.57 (brs, 6H, CH₂CH₂, H-7'', H-8'') 3.25 (t, 4H, *J*₁, *J*₂ = 5.2 Hz, NCH₂, H-6''), 5.73 (p, 1H, H-1), 6.93 (d, 2H, *J* = 8.8 Hz, H-4''), 7.25 (t, 1H, *J*₁, *J*₂ = 6.8 Hz, *J*₂ = 7.6 Hz, H-5'), 7.35 (t, 2H, *J*₁, *J*₂ = 7.6 Hz, H-4'), 7.43 (d, 2H, *J* = 7.6 Hz, H-3'), 7.62 (d, 2H, *J* = 8.8 Hz, H-3''), 7.99 (s, 1H, H-1''), 8.42 (d, 1H, *J* = 9.2 Hz, H-4), 11.36 (s, 1H, H-2); ¹³C NMR (100 MHz, DMSO-*d*₆): δ 21.90 (C-6'), 24.36 (CH₂, C-8''), 25.04 (CH₂, C-7''), 48.18 (NCH₂, C-6'') 52.71 (C-1'), 113.65 (C-4''), 123.57 (C-2''), 126.78 (C-5'), 127.16 (C-3'), 128.67 (C-4'), 129.16 (C-3''), 143.68 (C-2'), 144.44 (C=N, C-1''), 152.79 (C-5''), 176.21 (C=S, C-3). Anal. Calcd. for C₂₁H₂₆N₄S: C, 68.82; H, 7.15; N, 15.29; S, 8.75%. Found: C, 68.88; H, 7.07; N, 15.36; S, 8.67%.

Chirality DOI 10.1002/chir

Cell Culture

Human breast adenocarcinoma (MCF-7), human alveolar adenocarcinoma (A549), human cervix adenocarcinoma (HELA), and human stomach adenocarcinoma (HGC-27) cells were maintained in Dulbecco's Modified Eagle Medium (DMEM; Sigma, St. Louis, MO) containing 10% fetal calf serum (Thermo, Waltham, MA), 100 IU of penicillin/mL, and 100 µg/mL of streptomycin (both from Life Technologies, Rochester, NY).

Cell Viability Assay

Cells were seeded at 5 × 10⁴ cells/mL of a 24-well cell culture plate and incubated for 48 h. After 48 h incubation, the cells were treated with a different concentration (2.5, 10, 50, and 100 µM) of compounds for 24 h. Cell viability was determined by MTT (3-[4,5-dimethylthiazol-2-yl]-2,5-diphenyl-tetrazoliumbromide) assay. For the MTT assay, MTT solution (mg/mL) was added onto the cells (500 µl/well) and incubated for 1 h at 37°C. Absorbance was measured at 570 nm using an Epoch microplate spectrophotometer (BioTek Instruments, Winooska, VT).

Statistical Analyses

All of data were analyzed with an analysis of variance (ANOVA) test (prism 5 software). *P* < 0.05 was considered statistically significant.

Molecular Modeling Study

In an effort to explain the possible mechanism by which the new chiral thiosemicarbazone derivative (**17b**) displayed antiproliferative activity toward HGC-27 and guide further SAR studies, the preferential pharmacophore modeling was carried out via Discovery Studio (DS; Accelrys Software, San Diego, CA) 3.5. Compound **17b** was designed and minimized using the conjugate gradient algorithm with the help of DS 3.5.¹⁹ Afterwards, to generate conformations a subprotocol of DS 3.5 was applied to determine the stable conformations of the mentioned compound. We determined the stable two forms of the compound as listed in Table 1.

Pharmacophore Generation

The results of the SAR study reported that compound **17b** was more active than the others and also the reference compound against HGC-27 cells. Hence, we attempted to determine its pharmacophore model. In this study, HipHop,^{20,21} which is one method of a pharmacophore model, was used for the mentioned reasons. HipHop provides a feature-based alignment of an active compound. Furthermore, the chemical features of the molecule were superimposed against the reference compound using the HipHop method. Conformational models of the compound **17b** were investigated in this application.

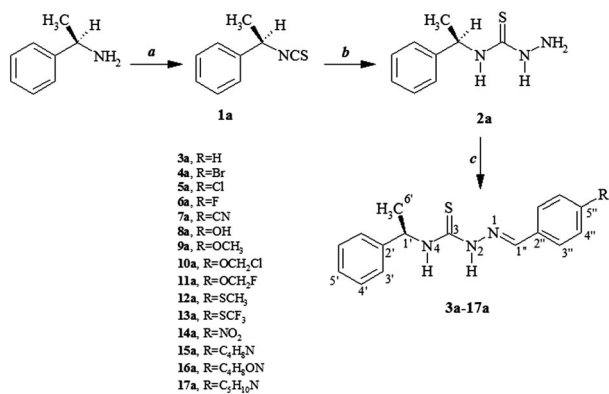
RESULTS AND DISCUSSION

Chemistry

The synthesis of the target chiral thiosemicarbazones was accomplished using the reaction sequence in Scheme 1. The chiral isothiocyanates (**1a-b**) as key intermediates were synthesized by treatment of (R)-(+)-α-methylbenzylamine and (S)-(-)-α-methylbenzylamine with CSCl₂ in the presence of NaOH in a water–chloroform medium at 0°C for 24 h, as described in previously reported methods.²² Thus, the chiral center from chiral amines was retained. Subsequently, chiral thiosemicarbazides (**2a-b**) were prepared by reacting hydrazine monohydrate with chiral isothiocyanates (**1a-b**) in diethylether at room temperature.²³ A series of chiral thiosemicarbazones (**3a-17a** and **3b-17b**) as an enantiomeric pair were synthesized by refluxing an equimolar ratio of the *p*-substituted benzaldehydes and chiral thiosemicarbazides in methanol medium without using a catalyst. The reactions were followed until complete consumption of thiosemicarbazides. The novel chiral thiosemicarbazones (**3a-17a** and **3b-17b**) were obtained in good yields (69–87%) and high enantiopurity after recrystallization from ethanol.

TABLE 1. IC₅₀ values (in μM) for chiral thiosemicarbazones

Compound	R	Cancer cell lines			
		MCF-7 (Breast)	A549 (Lung)	HeLa (Cervix)	HGC-27 (Stomach)
3a	-H	>100	20.1	>100	12.5
3b	-H	>100	16.9	>100	13.4
4a	-Br	>100	>100	>100	>100
4b	-Br	>100	>100	>100	>100
5a	-Cl	>100	>100	>100	>100
5b	-Cl	>100	>100	>100	>100
6a	-F	>100	>100	>100	>100
6b	-F	>100	>100	>100	43.5
7a	-CN	>100	>100	>100	>100
7b	-CN	>100	>100	>100	>100
8a	-OH	24.6	>100	45.7	40.3
8b	-OH	>100	42.2	42.8	46.9
9a	-OCH ₃	>100	>100	>100	>100
9b	-OCH ₃	>100	>100	>100	>100
10a	4-chlorophenoxy	>100	>100	46.4	>100
10b	4-chlorophenoxy	>100	>100	38.0	>100
11a	4-fluorophenoxy	>100	>100	>100	>100
11b	4-fluorophenoxy	>100	>100	48.8	>100
12a	-SCH ₃	>100	>100	>100	>100
12b	-SCH ₃	>100	>100	>100	>100
13a	-SCF ₃	48.6	>100	>100	>100
13b	-SCF ₃	>100	>100	>100	>100
14a	-NO ₂	>100	>100	>100	>100
14b	-NO ₂	>100	>100	>100	>100
15a	-prryolidine	>100	>100	>100	>100
15b	-prryolidine	>100	>100	>100	>100
16a	-morpholine	>100	>100	>100	>100
16b	-morpholine	>100	>100	>100	48.2
17a	-piperidine	>100	>100	>100	>100
17b	-piperidine	>100	>100	>100	4.6
Taxol (Sindaxel)		7.65	7.56	9.6	10.3



Scheme 1. Synthesis of thiosemicarbazones in (R)-enantiomeric form. Reagents and conditions: (a) CSCl₂, NaOH/water, CHCl₃, rt, 24 h; (b) NH₂NH₂·H₂O (98%), Et₂O, rt, 24 h; (c) 4-substitutedbenzaldehydes, CH₃OH, reflux, 10–12 h.

All thiosemicarbazones (**3a-17a** and **3b-17b**) were characterized by the combined use of UV-vis, IR, ¹H NMR, ¹³CNMR, 2D NMR, and MS spectral data. In the IR spectra

of chiral thiosemicarbazones (**3a-17a** and **3b-17b**), stretching vibrations attributed to the $\nu(\text{N-H})$ at 3309–3372 cm^{-1} and 3124–3196 cm^{-1} were observed, while the characteristic intense bands at 1591–1609 cm^{-1} and 1200–1238 cm^{-1} were attributed to $\nu(\text{C=N})$ and $\nu(\text{C=S})$, respectively. It was suggested that in the solid phase the thiosemicarbazones will be retained in the thione form. The ¹H NMR spectra of chiral thiosemicarbazones (**3a-17a** and **3b-17b**) showed a singlet peak attributable to the –NH (H-2) proton in the range δ 11.27–11.87 ppm as well as a singlet peak attributable to the –NH (H-4) proton in the range δ 8.33–8.89 ppm. The signal of the azomethine proton (H-1'') appeared as a singlet at δ 7.98–8.19 ppm. All aromatic protons were observed with the expected chemical shifts and coupling constants. The proton at the chiral center was observed at δ 5.72–5.77 ppm as a pentet peak. The ¹³C NMR spectra of the thiosemicarbazones exhibited two important signals at δ 175.71–177.22 and at δ 143.68–144.50 ppm attributed to the thioamide (C=S) and imine (C=N) carbon atoms, respectively. The signals at δ 112.01–164.73 ppm in the spectra were attributed to the aromatic carbons. The signal at δ 53.31–52.02 ppm was attributed to the chiral carbon atom. MS

spectra of all chiral thiosemicarbazones were in line with the proposed structures.

Antiproliferative Activity Assays

In order to assess any possible toxic effects of the compounds they were evaluated according to the MTT assay. The serial dilutions 2.5, 10, 50, and 100 μM of the compounds were incubated with HeLa, A549, MCF-7, and HGC-27 cell lines for 24 h. Sindaxel is an anticancer drug used as a control group. The compounds of **8a** (IC_{50} 45.7 μM), **8b** (IC_{50} 42.8 μM), **10a** (IC_{50} 46.4 μM), **10b** (IC_{50} 38.0 μM), and **11b** (IC_{50} 48.8 μM) showed weaker activity than the reference drug (IC_{50} 9.6 μM) on HELA cells. Similarly, the compounds **6b** (IC_{50} 43.5 μM), **8a** (IC_{50} 40.3 μM), and **8b** (IC_{50} 46.9 μM) showed less cytotoxic effect by comparison with sindaxel (IC_{50} 10.3 μM) on the HGC-27 cell line. Sindaxel (IC_{50} 7.56 μM and IC_{50} 7.65 μM) showed a better cytotoxic effect than compounds **8b** (IC_{50} 42.2 μM) and **13a** (IC_{50} 48.6 μM) on A549 and MCF-7 cell lines, respectively. On the other

hand, the IC_{50} value of compound **8a** (24.6 μM) was measured on MCF-7 cells as well (Fig. 2), whereas compound **8a** has no potential effects on A549 cells. The IC_{50} values of **3a** were evaluated on A549 and HGC-27 as 20.1 μM and 12.5 μM , respectively (Fig. 1). The activity of **3b** against HGC-27 and A549 cells were assessed as mean IC_{50} values of 16.9 μM and 13.4 μM , respectively (Fig. 1). The greatest reduction of the maximum dose shown by **17b** was against the HGC-27 cell line. Compound **17b** showed a more prominent inhibitory effect (IC_{50} 4.6 μM) than the reference drug, Sindaxel (IC_{50} 10.3 μM) (Fig. 2). But interestingly, compound **17a** had no significant cytotoxic effect on any of the cell lines. Compound **17b** will be selected as a promising candidate for further development. IC_{50} (μM) values are listed in Table 1.

Structure-Activity Relationship Study

The SAR studies were applied to define how the substituent on the benzene ring and chiral structures of thiosemicarbazone derivatives (**3a-17a** versus **3b-17b**) involved the

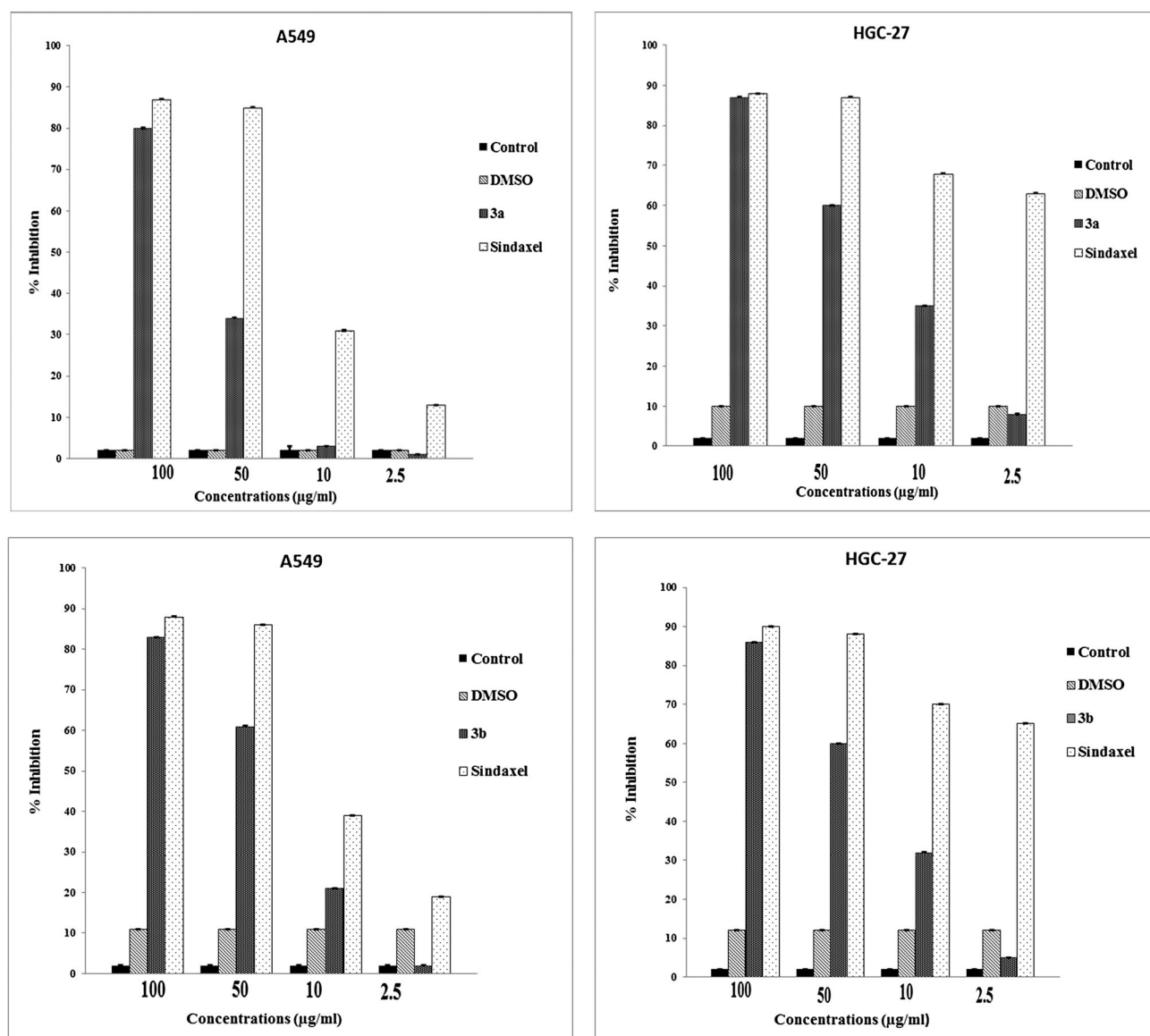


Fig. 1. Cell viability of compounds: Effect of compound **3a** and **3b** against A549 and HGC-27 cell lines.

anticancer activity. Compounds **3a** and **3b** have the same backbone, but different stereochemistry. These compounds without any substituent group on the benzene ring show antiproliferative activities against the A549 and HGC-27 cells. In this part of the study, the effect of the different substituent group(s) on the benzene ring of compounds **3a** and **3b** were evaluated. First, we used electron-withdrawing groups such as $-\text{Br}$, $-\text{Cl}$, $-\text{F}$, $-\text{CN}$, $-\text{NO}_2$ instead of a hydrogen atom on the 3-position of the benzene ring. Compound **6b** exhibited activity against HGC-27 cells; however, the activity value (IC_{50} 43.5 μM) was less than compounds **3a-3b** (IC_{50} 12.5 and 13.4 μM) and also the reference compound, sindaxel (IC_{50} 10.3 μM). In addition, the electron-donor groups ($-\text{OH}$, OCH_3 , $-\text{OPhCl}$, $-\text{OPhF}$, $-\text{SCH}_3$, $-\text{SCF}_3$) were used under the same conditions. This time, compounds **10a**, **10b**, and **11b** exhibited poor activities, with IC_{50} values of 38.0–48.8 μM against HeLa cells, but not others. Furthermore, the pyrrolidine, morpholine, and piperidine groups were utilized to observe the activity change according to compounds **3a-3b** and the reference compound. Compound **17b** was the most potent of all the compounds and the reference compound, which indicated that the exchange of the piperidine group including the S form of the chiral thiosemicarbazone improved the antiproliferative activity against HGC-27 cells. Compared with **17b**, compound **17a**, with a bulky substituent which connected with the chiral carbon, had more potent activity. The substituent in the benzene ring and R- and S- nomenclature of the chiral carbon widely influenced the activity. Moreover, all of the thiosemicarbazone derivatives showed low activity toward MCF-7, A549, and HeLa. Thus, compound **17b** exhibited HGC-27 selectivity.

Pharmacophore Generation

In the present study, the HipHop was used to form a pharmacophore hypotheses to elucidate the specification of the SARs of the pharmacophore sites of the novel chiral thiosemicarbazone, **17b**. The obtained hypotheses could be correlated with the activity of the mentioned molecule. Compound **17b** exhibited 2-fold more antiproliferative activity than the reference compound against HGC-27 cells (Table 1). According to the results of the antiproliferative activities of the thiosemicarbazone derivatives, the most active molecule,

17b, shown in Figure 3, was used to derive common feature-based alignments. It is considered a reference compound (Fig. 3) and **17b** with a principal value of 2 and maximum omitting features (MaxOmitFeat) value of 0. Then 10 pharmacophore hypotheses were generated from compound **17b** using the Auto Pharmacophore Generation protocol in Discovery Studio 3.5. Within the generated 10 hypotheses, the hypothesis in Figure 4A was determined for future steps. These features were one Hb-Acceptor, one Hb-Donor, two hydrophobic, and two ring aromatic in 10 pharmacophore models. Figure 4A–D and Figure 5E were projected as the common feature functions to elucidate the pharmacophore site of compound **17b**. In addition, Figure 4C lists the mapping of **17b** on the anticipated pharmacophore model meant for the most active molecule. The reference compound, sindaxel, was also investigated to compare it with the mentioned compound **17b** by using pharmacophore modeling subprotocol of DS 3.5. We first defined the pharmacophore model of sindaxel and then the possible conformations occurring via the generate conformation subprotocol of DS 3.5. Finally, the best model was chosen to evaluate the differences with compound **17b**, which has six features containing four Hb-Donors, one hydrophobic, and one ring Aromatic, possessing the highest ranking score in Figure 5F,G.

The generated pharmacophore models showed that the two hydrophobic features were found to be significant for antiproliferative activity. Two hydrophobic features indicated the appropriate active shape of the molecule. This molecule showed the required placement of bulky ring moieties. The two hydrophobic atoms or groups at the defined positions

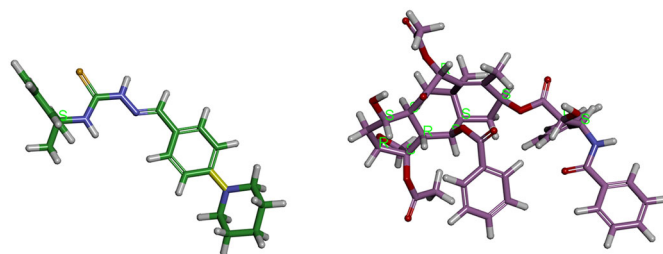


Fig. 3. The 3D chemical structures of the compound **17b** and reference compound, sindaxel, respectively.

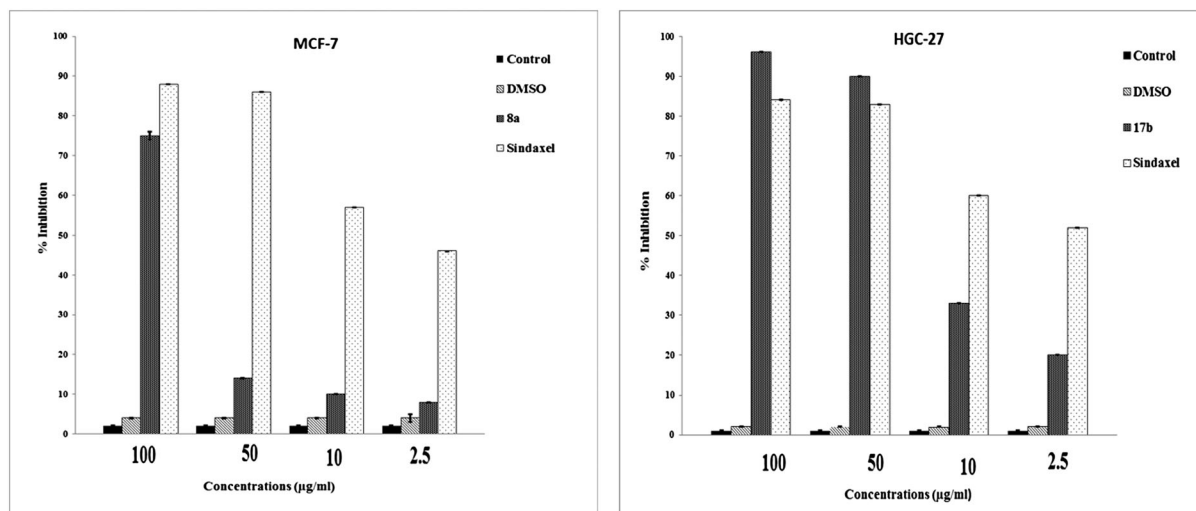


Fig. 2. Cell viability of compounds: Effect of compound **8a** against MCF-7 cell line and effect of compound **17b** against HGC-27 cell line.

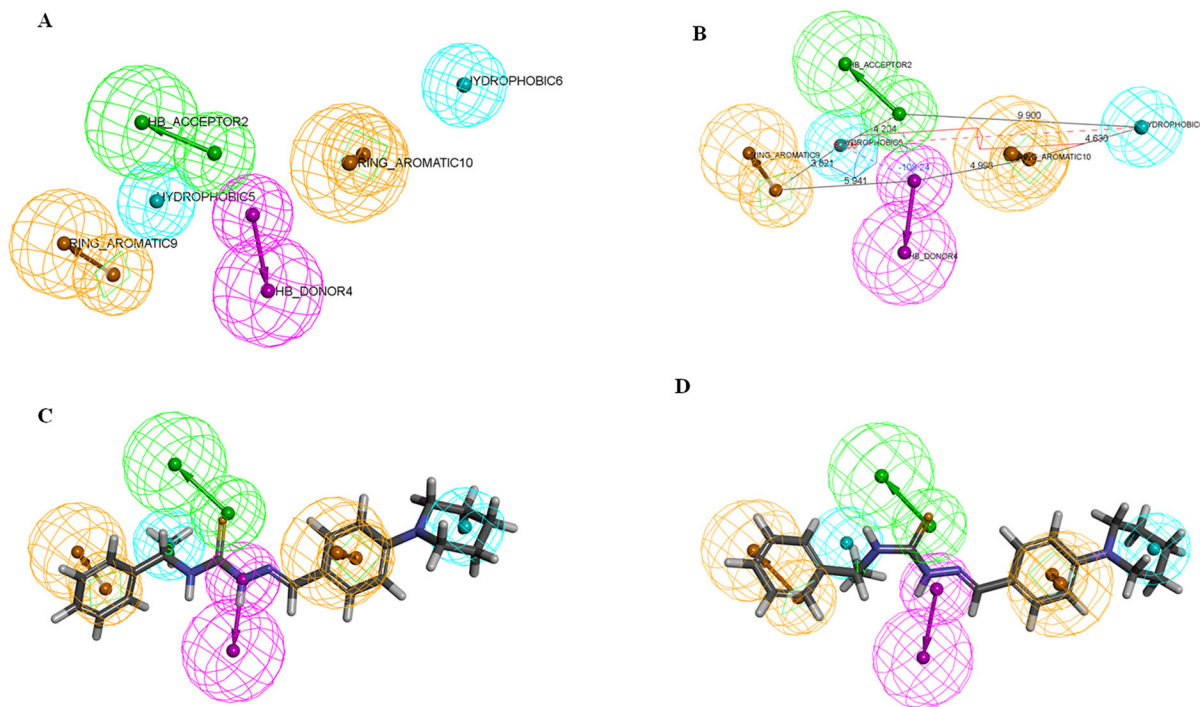


Fig. 4. **A.** Anticipated pharmacophore model generated for HGC-27 cell inhibitor activity of tested thiosemicarbazone derivatives. **B.** Distance and torsional angles between the generated common features calculated in the participated pharmacophore model. Alignment of the 3D generated conformer structures of compound **17b** as the reference AdeABC efflux pump inhibitors. **C.** Pharmacophore mapping of the compound **17b**. **D.** Pharmacophore mapping of the compound **17a**.

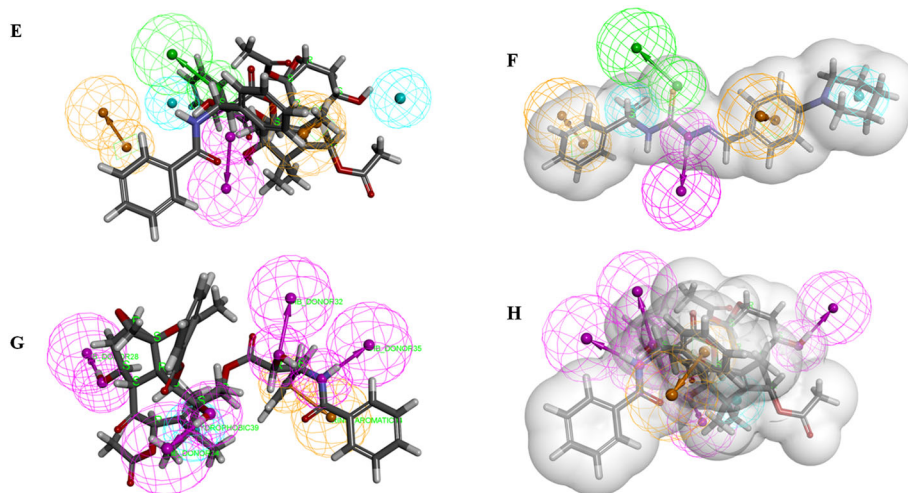


Fig. 5. **E.** Pharmacophore mapping of reference compound, sindaxel less active than compound **17b**. **F.** The generated slab of the anticipated pharmacophore model with the compound **17b**. **G.** Anticipated pharmacophore model generated for HGC-27 cell inhibitor activity of the reference compound, sindaxel. **H.** The generated slab of the anticipated pharmacophore model with the reference compound, sindaxel.

were necessary in the molecule to show antiproliferative activity against HGC-27 cells and bind to the target protein.

All novel chiral thiosemicarbazone derivatives with their conformational models were mapped onto the generated HipHop pharmacophore model using a "rigid" fitting method and "best mapping only" option to obtain the bioactive conformation of each molecule in the Ligand Pharmacophore Mapping protocol in Discovery Studio 3.5. The results of mapping of the features onto the compounds are given in Table 2, and compound **17b**, which was experimentally found as the most active chiral thiosemicarbazone derivative, showed the best fit value of 6.000 for the generated pharmacophore *Chirality* DOI 10.1002/chir

hypothesis, fitting all the mapped common features in the anticipated model with a specified "Pharmprint" value of 11111.

Additionally, the novel chiral thiosemicarbazone derivatives were substituted with a piperidine group instead of the hydrogen atom at 3-position of the benzene ring, and compound **17b** possessed a better match with all the features in the anticipated model in Figure 3C. When compound **17b** was also compared with compound **17a**, we observed that the (S)-enantiomer (**17b**) was better matched than the (R)-enantiomer (**17a**) (see Fig. 3D). This shows that the (R)- and (S)-enantiomer greatly influenced the activity.

TABLE 2. Alignment of common-feature pharmacophore model with test set

Compound	Fit Value
3a	No map found
3b	No map found
4a	2.05092
4b	5.25537
5a	1.93746
5b	5.19604
6a	No map found
6b	No map found
7a	No map found
7b	No map found
8a	No map found
8b	No map found
9a	2.2815
9b	5.15034
10a	2.37954
10b	4.88218
11a	2.10885
11b	5.30328
12a	3.20682
12b	5.25216
13a	2.07216
13b	5.31915
14a	No map found
14b	No map found
15a	3.82272
15b	5.35914
16a	2.26292
16b	5.32714
17a	2.78772
17b	6.00000
Sindaxel	No map found

As mentioned, compound **17b** exhibited 2-fold more anti-proliferative activity than the reference compound against HGC-27 cells (Table 1). Hence, pharmacophore model was also generated for the reference compound, sindaxel, to elucidate this state. The obtained pharmacophore model was better matched with compound **17b**; however, the reference compound was not able to show any match with the determined pharmacophore model, as given in Figure 3E. This observation explains why the *(S)*-(+)-2-[(4-piperidin-1-yl)benzylidene]-*N*-(1-phenylethyl)hydrazine carbothioamide (**17b**) structure is more favorable than sindaxel for increasing the potency in this set of compounds.

CONCLUSION

Here we synthesized a series of novel chiral thiosemicarbazones derived from homochiral amines in both enantiomeric forms and evaluated their in vitro antiproliferative activity against the A549, MCF-7, HeLa, and HGC-27 cell lines. Sindaxel showed much stronger activity against the MCF-7, A549, HeLa cancer cells, but did not show good activity against HGC-27 cells, according to compound **17b** in this study. If we can investigate the 3D chemical structures of these compounds, we can see that they many differences, such as atom, molecular weight, conformation, etc. It is known that these properties are very effective in determining and evaluating the activity of any compound against any cell. Because of this, we examined the SAR study of the compounds in this study. In other words, the SAR studies were

used to define how the substituent on the benzene ring and chiral structures of thiosemicarbazone derivatives (**3a-17a** versus **3b-17b**) involved the anticancer activity. In conclusion, the generated 3D common feature pharmacophore hypothesis showed that the conformational properties and substituent groups of the compounds were significant for antiproliferative activity against any cells. In addition, the compound possessing the *(S)*-(+)-2-[(4-piperidin-1-yl)benzylidene]-*N*-(1-phenylethyl)hydrazinecarbothioamide (**17b**) structure was important for improving HGC-27 inhibitor potency, rather than (*2a,5b,7b,10b,13a*)-4,10-Diacetoxy-13-[(2*R,3S*)-3-(benzoylamino)-2-hydroxy-3-phenylpropanoyl]oxy-1,7-dihydroxy-9-oxo-5,20-epoxytax-11-en-2-yl benzoate (*sindaxel*) (see Figs. 4C, 5E) in these attempted thiosemicarbazone derivatives.

ACKNOWLEDGMENTS

This work was supported by the Scientific Research Projects Governing Unit Council of Scientific Research Projects (Grant no. FEF 12.15), Gaziantep, Turkey. The authors thank Esin Akı Yalcin and the research group for technical assistance.

LITERATURE CITED

1. Cho JY. Molecular diagnosis for personalized target therapy in gastric cancer. *J Gastric Cancer* 2013;13:129–135.
2. Boulikas T, Vougiouka M. Cisplatin and platinum drugs at the molecular level. (review). *Oncol Rep* 2003;10:1663–1682.
3. da Silva AP, Martini MV, de Oliveira CM, Cunha S, de Carvalho JE, Ruiz AL, da Silva CC. Antitumor activity of (–)-alpha-bisabolol-based thiosemicarbazones against human tumor cell lines. *Eur J Med Chem* 2010;45:2987–2993.
4. Tian J, Peehl DM, Zheng W, Knox SJ. Anti-tumor and radiosensitization activities of the iron chelator Hdp44mT are mediated by effects on intracellular redox status. *Cancer Lett* 2010;298:231–237.
5. Richardson DR, Kalinowski DS, Lau S, Jansson PJ, Lovejoy DB. Cancer cell iron metabolism and the development of potent iron chelators as anti-tumour agents. *Biochim Biophys Acta* 2009;1790:702–717.
6. Richardson DR. Iron chelators as therapeutic agents for the treatment of cancer. *Crit Rev Oncol Hematol* 2002;42:267–281.
7. Kashyap M, Kandeekar S, Baviskar AT, Das D, Preet R, Mohapatra P, Satapathy SR, Siddharth S, Guchhait SK, Kundu CN, Banerjee UC. Indenoindolone derivatives as topoisomerase II-inhibiting anticancer agents. *Bioorg Med Chem Lett* 2013;23:934–938.
8. Dilovic I, Rubcic M, Vrdoljak V, Kraljevic Pavelic S, Kralj M, Piantanida I, Cindric M. Novel thiosemicarbazone derivatives as potential antitumor agents: Synthesis, physicochemical and structural properties, DNA interactions and antiproliferative activity. *Bioorg Med Chem* 2008;16:5189–5198.
9. Yalowitz JC, Wu X, Zhang R, Kanagasabai R, Hornbaker M, Hasinoff BB. The anticancer thiosemicarbazones Dp44mT and triapine lack inhibitory effects as catalytic inhibitors or poisons of DNA topoisomerase IIalpha. *Biochem Pharmacol* 2012;84:52–58.
10. Wu CP, Shukla S, Calcagno AM, Hall MD, Gottesman MM, Ambudkar SV. Evidence for dual mode of action of a thiosemicarbazone, NSC73306: a potent substrate of the multidrug resistance linked ABCG2 transporter. *Mol Cancer Ther* 2007;6Pt 1):3287–3296.
11. Moitra K, Lou H, Dean M. Multidrug efflux pumps and cancer stem cells: insights into multidrug resistance and therapeutic development. *Clin Pharmacol Ther* 2011;89:491–502.
12. Smith SW. Chiral toxicology: it's the same thing...only different. *Toxicol Sci* 2009;110:4–30.
13. McConathy J, Owens MJ. Stereochemistry in drug action. *prim care companion. J Clin Psychiatry* 2003;5:70–73.
14. Caner H, Groner E, Levy L, Agranat I. Trends in the development of chiral drugs. *Drug Discov Today* 2004;9:105–110.
15. Nguyen LA, He H, Pham-Huy C. Chiral drugs: an overview. *Int J Biomed Sci* 2006;2:85–100.
16. Nunez MC, Garcia-Rubino ME, Conejo-Garcia A, Cruz-Lopez O, Kimatrai M, Gallo MA, Espinosa A, Campos JM. Homochiral drugs: a demanding tendency of the pharmaceutical industry. *Curr Med Chem* 2009;16:2064–2074.

17. Hutt AJ. Chirality and pharmacokinetics: an area of neglected dimensionality? *Drug Metabol Drug Interact* 2007;22:79–112.
18. Vandresen F, Falziroli H, Almeida Batista SA, da Silva-Giardini AP, de Oliveira DN, Catharino RR, Ruiz AL, de Carvalho JE, Foglio MA, da Silva CC. Novel R-(+)-limonene-based thiosemicarbazones and their antitumor activity against human tumor cell lines. *Eur J Med Chem* 2014;79:110–116.
19. Accelrys Software Inc AS. Discovery Studio 3.5. San Diego, CA; 2013.
20. Krovat EM, Fruhwirth KH, Langer T. Pharmacophore identification, in silico screening, and virtual library design for inhibitors of the human factor Xa. *J Chem Inf Model* 2005;45:146–159.
21. Yildiz I, Ertan T, Bolelli K, Temiz-Arpaci O, Yalcin I, Aki E. QSAR and pharmacophore analysis on amides against drug-resistant *S. aureus*. *SAR QSAR Environ Res* 2008;19:101–113.
22. Karakucuk-Iyidoğan A, Tasdemir D, Oruc-Emre EE, Balzarini J. Novel platinum(II) and palladium(II) complexes of thiosemicarbazones derived from 5-substitutedthiophene-2-carboxaldehydes and their antiviral and cytotoxic activities. *Eur J Med Chem* 2011;46:5616–5624.
23. Karaküçük-Iyidoğan A, Mercan Z, Oruç-Emre EE, Taşdemir D, İşler İ, Kılıç İH, Özaslan M. Synthesis, characterization, and biological evaluation of some novel thiosemicarbazones as possible antibacterial and antioxidant agents. *Phosphorus Sulfur Silicon Relat Elem* 2014;189:661–673.